Performance of Density Functional Theory on the Potential-Energy Surface of the H + OCS System

Betsy M. Rice,* Sharmila V. Pai,† and Cary F. Chabalowski

U.S. Army Research Laboratory, Aberdeen Proving Ground, Maryland 21005-5066

Received: March 30, 1998; In Final Form: June 12, 1998

The H + OCS potential-energy surface (PES) was used to evaluate the performance of density functional theory by comparing the results to ab initio calculations at the QCISD(T)//UMP2 and UMP2 levels using the aug-cc-pVTZ and 6-311+G(2df, 2p) basis sets. The two major reaction paths on this PES involve formation of $OH(^2\Pi)$ + $CS(^1\Sigma)$ (reaction I) and $SH(^2\Pi)$ + $CO(^1\Sigma)$ (reaction II). Experimental and QCISD(T)//UMP2/aug-cc-pVTZ activation barriers for (II) and reaction enthalpies for (I) and (II) were compared to values calculated by several density functionals (BLYP, B3LYP, B3PW91, BPW91, BP86, and B3P86) using the aug-cc-pVTZ basis set. All DFT/aug-cc-pVTZ predictions, except for the B3LYP prediction of the enthalpy of reaction I, were outside the range of experimental uncertainty. B3LYP predictions were in closest agreement with the experimental values and QCISD(T) predictions. B3LYP, BPW91, and B3PW91 predictions of the rate-limiting barrier to reaction II are within 3.5 kcal/mol of the QCISD(T) prediction, and all DFT values are below that of the QCISD(T). Reaction enthalpies for (I) and (II) were calculated using the BHandHLYP density functional and the 6-311+G(2df,2p) basis set. These predictions were closer to experiment and QCISD(T) values than any other DFT calculations, and the predicted enthalpy for reaction I is within the range of experimental values. The second portion of the study compared B3LYP and BLYP predictions of the 12 transition states and 6 stable intermediates within this PES with previously reported QCISD(T)//UMP2/6-311+G(2df,2p) predictions. The complexity of this surface allows for the evaluation of barrier heights for 28 reactions involving hydrogen addition, elimination, isomerization, migration, and radical diatomic elimination. With the exception of five reactions, all B3LYP barrier heights are within 3.7 kcal/mol of the QCISD(T) predictions and in several cases are in as good or better agreement than the UMP2 predictions. In addition, all but one of the B3LYP barriers lie below the QCISD(T) values. The most significant differences between the ab initio and DFT predictions were in the saddle points for radical elimination or addition. BLYP/6-311+G(2df, 2p) failed to find the two transition states associated with SH elimination from the *cis*- and *trans*-HSCO species. B3LYP located the saddle point for SH elimination from *cis*-HSCO, but its prediction of a saddle-point structure for SH elimination from *trans*-HSCO has an energy (without zero-point corrections) lower than that of the products. These transition states were subsequently optimized using the BHandHLYP functional and the 6-311+G(2df,2p) and 6-31G** basis sets. The geometries of these saddle points were in better agreement with UMP2/6-311+G(2df,2p) predictions than were the BLYP and B3LYP predictions. The BLYP predictions are in overall worse agreement with the QCISD(T) results than are the B3LYP predictions.

I. Introduction

Density functional theory (DFT) is gaining acceptance as a standard research tool for the study of chemical reactions. Generalized gradient approximation (GGA) DFT has been shown to predict properties of stable covalently bound molecules with reasonable accuracy while using a fraction of the computational resources required for other ab initio treatments at correlated levels.[1−6] Unfortunately, DFT investigations of transition states (particularly those involving hydrogen)[7−18] and noncovalently bound complexes (i.e., hydrogen-bonded or van der Waals species)[19−30] have not shown a consistent pattern of performance. Some studies suggest that DFT reasonably predicts properties and energetics of critical points located along reaction paths.[9,11−14,16−18] Other studies have clearly shown that in some cases, DFT fails at adequately describing or even predicting the existence of extrema on a potential-energy surface (PES).[7−10,12,14−16] Given these inconsistencies in performance, it is clear that applications of DFT to reaction paths must be performed in order to understand and establish the limits of the theory in the study of chemical reactions.

Toward this end, we present results of DFT predictions of the H + OCS PES and compare them against our earlier predictions determined by ab initio theory using levels of correlation as high as QCISD(T) and basis sets as large as aug-cc-pVTZ.[31,32] The agreement of our earlier theoretical predictions with experimental information suggests that the ab initio predictions are suitable metrics against which a comparison with DFT can be made. Additionally, the complexity of the H + OCS PES makes it an attractive system for testing the performance of GGA DFT in that several types of reactions can be examined within the same chemical system.

† National Research Council Postdoctoral Fellow at the U.S. Army Research Laboratory.

S1089-5639(98)01671-5
Published on Web 08/08/1998

The H + OCS system has two major reaction channels

$$H(^2S) + OCS(^1\Sigma) \rightarrow OH(^2\Pi) + CS(^1\Sigma) \quad \Delta H^\circ_{298} = 57.3 \text{ kcal/mol} \quad \text{(I)}$$

$$H(^2S) + OCS(^1\Sigma) \rightarrow SH(^2\Pi) + CO(^1\Sigma) \quad \Delta H^\circ_{298} = -11.5 \text{ kcal/mol} \quad \text{(II)}$$

and many critical points along the two paths.[31,32] These critical points include 12 saddle points and 6 stable four-body intermediates. Of the stable intermediates, five are covalently bound species and one is a weakly bound complex of the products of reaction I. At least 28 reactions can occur on the PES including hydrogen addition and elimination, hydrogen migration, isomerization, and elimination/addition reactions involving the diatomic radicals OH and SH. Testing the performance of DFT within such a system will add more data points to help determine the types of reaction barriers that DFT can (or cannot) describe.

The earlier ab initio calculations predicted that the highest barrier along the low-energy path for reaction II involves the formation of *cis*-HSCO from the reactants H + OCS.[31,32] Our best prediction of the zero-point-corrected barrier is within 2 kcal/mol of the reported experimental activation energy (not including tunneling effects). The agreement with experiment indicates that this level of theory (QCISD(T)//UMP2/aug-cc-pVTZ) is a satisfactory level to describe this system. Thus, we use the QCISD(T)//UMP2/aug-cc-pVTZ energy predictions as a standard against which to measure the performance of GGA density functional theory for the hydrogen addition reactions. Additionally, the reaction enthalpies calculated at QCISD(T)//UMP2-aug-cc-pVTZ are within the range of experimental values for reactions I and II and provide other metrics with which to compare the performance of DFT. The QCISD(T) results were chosen as the general metrics due to the lack of experimental data about other parts of the PES (such as the activation energy for reaction I or observation/characterization of the four-body reaction intermediates).

II. Methods

DFT calculations of critical points on the PES for H + OCS reactions were performed using the Gaussian 94 (G94) program package.[33] Two sets of calculations will be presented. In one set, geometry optimizations of all stable and transition-state species were done using the 6-311+G(2df,2p)[34] basis set and the BLYP and B3LYP density functionals.[35−38] These results will be compared to earlier ab initio UMP2 and QCISD(T)//UMP2/6-311+G(2df,2p) predictions.[31,32] In the second set, the barrier to formation of the *cis*-HSCO intermediate for reaction II was determined through geometry optimizations using the BLYP, B3LYP, BPW91, B3PW91, BP86, and B3P86 density functionals[35−40] and the aug-cc-pVTZ[41] basis set. The density functionals represent various corrections to the local spin density approximation (LSDA) functional done with the LSDA exchange and the Vosko, Wilk, and Nusair correlation functional (VWN).[35] The corrections use either the gradient-corrected exchange functional of Becke (B)[36] or the hybrid three-parameter functional proposed by Becke, which is composed of contributions from the exact Hartree−Fock, GGA, and Slater exchanges (B3).[37] The correlation functionals include corrections to VWN proposed by Lee, Yang, and Parr (LYP),[38] Perdew (P86),[39] and Perdew and Wang (PW91).[40] Additionally, selected critical points were characterized using the hybrid Becke-Half-and-Half-LYP (denoted as "BHandHLYP") functional,[33] which contains a larger contribution from the Hartree−Fock exchange than that of the B3 exchange functional. Comparisons are then made to previous ab initio predictions at the QCISD(T)//UMP2/aug-cc-pVTZ level.[31] All DFT calculations were performed using the default grid size given in G94. All geometry optimizations met the default convergence criteria given by G94. Normal-mode analyses were performed on all critical points to confirm that they were either transition states or minima.

BLYP/6-311+G(2df,2p) intrinsic reaction coordinate (IRC) calculations leading from all transition states were attempted. BLYP/6-311+G(2df,2p) failed to locate two of the saddle points located at the QCISD(T) level; these are the barriers to SH elimination reactions. These saddle points were located using the B3LYP functional; however, one of them (elimination of SH from *trans*-HSCO) had an energy that was lower than that of the product asymptotes, and its imaginary frequency was only 38i cm^{-1}. For these cases, IRC calculations using the B3LYP functional were performed but were successful only for the saddle point associated with the elimination of SH from *cis*-HSCO. The IRC calculations were terminated when minima were reached as defined by the default convergence criteria of the G94 set of programs. In cases where the IRC terminated due to an inability to satisfy the convergence criteria, a geometry optimization was attempted beginning with the final optimized structure of the IRC in order to establish the connecting minima.

III. Results and Discussion

A. Comparisons with Experiment. Quantitative experimental data for reactions of the H + OCS system that are available for comparison with theory are the thermal activation energy for reaction II and enthalpies for reactions I and II. These reaction enthalpies and barrier will be used to compare the performance of six density functionals using the aug-cc-pVTZ basis set. We have also included reaction enthalpies calculated with the 6-311+G(2df,2p) basis set and the BLYP, B3LYP, and BHandHLYP density functionals to assess the effect of the basis set.

Experimentally measured and theoretical values for the enthalpies of reactions I and II are given in Table 1. Values for the experimental reaction enthalpy for I range from 45.3 to 57.2 kcal/mol. Values for the experimental reaction enthalpy for II vary from −13.0 to −9.8 kcal/mol. The QCISD(T)//UMP2/aug-cc-pVTZ reaction enthalpies for I and II are 57.3 and −11.5 kcal/mol, respectively. DFT/aug-cc-pVTZ enthalpies for reaction I range from 61.3 to 69.6 kcal/mol. With the exception of the B3LYP prediction (i.e., 61.3 kcal/mol, which is within the error of one of the experimental values), all DFT/aug-cc-pVTZ predictions fall outside of the range of the measurements. The B3LYP prediction is in closest agreement with the QCISD(T)//UMP2/aug-cc-pVTZ value, followed by the BLYP prediction. Similarly, all DFT predictions of the reaction enthalpy for (II) are outside the range of experimental measurement, with the B3LYP prediction (−8.4 kcal/mol) in closest agreement with the experimental estimates and the QCISD(T)/aug-cc-pVTZ prediction. All other DFT/aug-cc-pVTZ predictions for this value are ∼5−10 kcal/mol smaller than the QCISD(T) prediction.

The experimental thermal activation energy for reaction II, which can be used as an approximate value with which to compare the calculated barriers, was determined by two groups. Tsunashima et al.[42] reports an activation energy of 3.9 kcal/mol, and Lee et al. [43] reports an activation energy of 3.85 kcal/mol. The zero-point-corrected QCISD(T)//UMP2/aug-cc-pVTZ prediction of the formation barrier to *cis*-HSCO is 5.7 kcal/mol without including tunneling effects. Zero-point-corrected

TABLE 1: Reaction Enthalpies and Zero-Point-Corrected Barrier to Formation of *cis*-HSCO (kcal/mol) Predicted Using the aug-cc-pVTZ Basis Set

	expt (kcal/mol)	ref	QCISD(T)// UMP2[b]	BLYP[b]	B3LYP[b]	BHand HLYP[b]	BP86	BPW91	B3PW91	B3P86
$\Delta H°_{298}$ (I)	45.3	44	57.3	63.7	61.3		67.2	69.6	65.6	65.0
	47.1	45	[59.8]	[64.7]	[62.2]	[56.4]				
	53.42	46								
	55 + 3.1	47								
	57.2 + 6.0	48								
$\Delta H°_{298}$ (II)	−9.8	42	−11.5	−4.4	−8.4		−0.8	1.9	−3.5	−4.6
	−9.8	49	[−8.8]	[−3.3]	[−7.2]	[−14.0]				
	−10.3 + 3.0	47								
	−10.45	45								
	−11.0	43								
	−11.3	44								
	−12.1 + 1.2	48								
	−13	46								
H + OCS → *cis*-HSCO	3.90 + 0.370[a]	42	5.7	0.7	2.2		0.1	2.4	3.0	1.0
	3.85 + 0.110[a]	43	5.7	0.7	2.2		0.1	2.4	3.0	1.0

[a] Activation energy extracted from rate measurements, includes tunneling effects. [b] Values in brackets correspond to results using the 6-311+G(2df,2p) basis set.

DFT predictions of this barrier underestimate the QCISD(T) value by ∼3−5 kcal/mol. The B3PW91 prediction of 3.0 is in closest agreement with the experimental values; however, it does not include tunneling effects, which we believe contribute to the experimental numbers. This implies that the B3PW91 value underestimates the correct classical barrier.

Reaction enthalpies for (I) and (II) were also evaluated using the 6-311+G(2df,2p) basis set and the density functionals BLYP, B3LYP, and BHandHLYP. The agreements of BLYP and B3LYP with QCISD(T) were worse than those using the aug-cc-pVTZ basis set. However, the BHandHLYP/6-311+G-(2df,2p) results were in closer agreement with experiment and QCISD(T) for both reactions than all other DFT calculations reported in this paper. Also, the BHandHLYP/6-311+G(2df,-2p) enthalpy for reaction I is within the range of experimental values.

B. Comparisons with QCISD(T). Although BLYP and B3LYP show no clear superiority to the other DFT methods in predicting the rate-limiting barrier for reaction II, they remain popular functionals that are being utilized by many groups. Additionally, there is evidence that indicates that B3LYP is a better functional for the description of critical points in some reactions.[18] Therefore, we evaluate their performance (as opposed to the remaining density functionals) in the second portion of this study. We will compare DFT/6-311+G(2df,-2p) critical points on the H + OCS potential-energy surface using the BLYP and B3LYP density functionals with the previously reported (QCISD(T)//MP2/6-311+G(2df,2p)) results. Also, a few critical points on the PES (structures **a**−**c**, **e**−**g**, **i**, **r**, **s**, and **u**) were characterized using the BHandHLYP density functional. Structures located using the UMP2/6-311+G(2df,-2p) basis set are illustrated in Figure 1; corresponding geometric parameters at the BLYP, B3LYP, BHandHLYP, and UMP2 levels are presented also. The BHandHLYP and UMP2 values are given in parentheses and brackets, respectively. Structures **r** and **s** could not be characterized using the BLYP functional. Calculated harmonic vibrational frequencies and geometric parameters for all of the critical points on the PES will be included in supplemental tables with limited discussion of this information. These properties have been analyzed in our previous studies;[31,32] therefore, this study will focus on the prediction of relative energies, with an emphasis on transition states, using DFT. The only substantial disagreements in geometric parameters from the earlier ab initio predictions[31,32] are in transition-state structures for the addition/elimination reactions (saddle points **j**, **l**, **n**, **r**, and **s** in Table 2) and correspond to the distances between the doublet and singlet fragments. These distances are 0.24−0.74 Å larger than the UMP2 predictions.

Six four-body stable intermediates have been located on the two paths for the H + OCS reactions and are described in Table 2. Saddle points leading to and from each local minima are also listed in Table 2 and characterized as one of the following reactions: (1) hydrogen addition or elimination, in which a new hydrogen bond is formed or broken; (2) isomerization, in which no bond is broken or made; (3) hydrogen migration, in which the hydrogen forms a new bond with another atom while breaking its bond with one atom in the complex; (4) radical diatomic addition or elimination, in which the fragments OH or SH are formed. Critical point **u** is described as a radical diatomic addition/elimination but has an element of an isomerization reaction. This transition state leads from the *trans*-HOCS minimum to that of a weakly bound linear intermediate with atomic arrangement SC···HO. The SC and HO moieties have bond lengths that are almost identical to those of the isolated diatomic products, and the C−H distance is ∼2.1 Å. The barrier to the formation of this intermediate is near the reaction endothermicity.

Table 2 gives zero-point-corrected energies of all of the critical points on the PES relative to the reactants H + OCS calculated using the 6-311+G(2df,2p) basis set and the QCISD-(T)//UMP2, UMP2, B3LYP, and BLYP levels. The relative energies of the critical points on the reaction paths are illustrated in Figure 2. BHandHLYP/6-311+G(2df,2p) geometry optimizations and normal-mode analyses were performed for stable structures **a**, **b**, **c**, **e**, **f**, **g**, and **i**; relative energies are also given in Tables 2 and 3. The BHandHLYP relative energies for the stable structures are in worse agreement with the QCISD(T) results than the B3LYP and BLYP predictions. The geometric parameters are similar to the MP2 values and are also provided in supplemental Tables 1 and 2. These structures were also optimized at the BHandHLYP/6-31G** level; all geometric parameters are within 2% of the BHandHLYP/6-311+G(2df,-2p) results. B3LYP predictions of the diatomic species are in much better agreement with QCISD(T)//UMP2 than both UMP2 and BLYP, and BLYP outperforms UMP2 by ∼5 kcal/mol or more. However, the BLYP predictions of the relative energies of the tetraatomic stable species are in better agreement with QCISD(T) predictions, except for species **i**. However, as noted above, species **i** is a weakly bound complex of the SC and HO

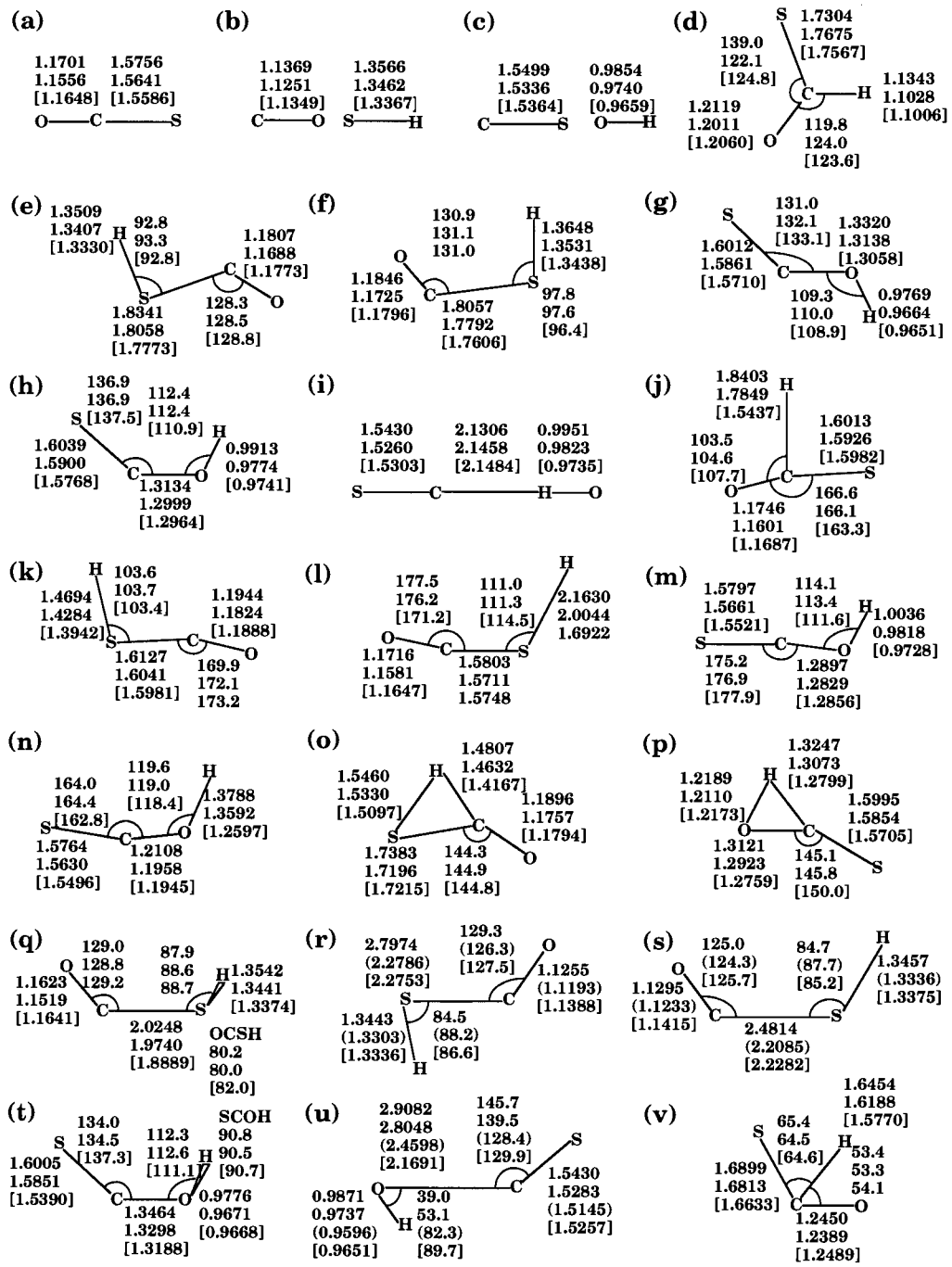

Figure 1. Structures and geometric parameters of stable and transition-state species on the H + OCS PES calculated using the 6-311+G(2df,2p) basis set. In each column of parameters, the uppermost value corresponds to the BLYP prediction and the second value corresponds to the B3LYP prediction. Structures **r** and **s** could not be characterized using the BLYP functional; thus, the uppermost values correspond to the B3LYP predictions. The values of the geometric parameters of structures optimized at the BHandHLYP and UMP2 levels are given in parentheses and brackets, respectively.

moieties and closely resembles the separated diatomic products of (I). Thus, the better agreement of the B3LYP prediction for this point is consistent with the behavior shown for the diatomic species. MP2 gives the worst agreement with the QCISD(T) energies for the tetraatomic species **d**−**i**.

Table 2 also gives the $\langle S^2 \rangle$ values for the critical points using the 6-311+G(2df,2p) basis set. Open-shell molecules, such as those presented here, can often be adequately described by post-Hartree−Fock methods if the spin contamination of the unrestricted Hartree−Fock zeroth-order wave function is small. In our earlier study, the largest UHF spin S^2 value of a critical point on the UMP2/6-311+G(2df,2p) PES is 0.89 compared to 0.75, the value associated with a doublet state.[31] As in the earlier study, we have used the spin S^2 value as a metric for the applicability of DFT to this system and have reported the S^2 values in Table 2. The S^2 values obtained from the DFT electron densities are no greater than 0.77, verifying that the converged densities are representative of doublet states.

Although the energies of the saddle point species relative to the reactants H + OCS are also given in Table 2, such information would be more useful in assessing the accuracy of the barrier heights if they were calculated relative to the minimum from which each reaction proceeds. This information is provided in Table 3. For the hydrogen addition reactions, UMP2 is in closest agreement with the QCISD(T) predictions, followed by B3LYP. As seen previously,[8,17,18] B3LYP under-

TABLE 2: Zero-Point-Corrected Energies and $\langle S^2 \rangle$ of Critical Points on the PES Relative to H + OCS (kcal/mol) Using the 6-311+G(2df,2p) Basis Set

		QCISD	MP2			B3LYP			BLYP			BH and HLYP		
critical point	description	(T)	energy	(diff)[a]	$<S^2>$	energy	(diff)[a]	$<S^2>$	energy	(diff)[a]	$<S^2>$	energy	(diff)[a]	$<S^2>$
b SH + CO	products of reaction II	−10.6	−0.3	(10.3)	0.76	−9.0	(1.6)	0.75	−5.0	(5.6)	0.75	−15.9	(−5.3)	0.76
c OH + CS	products of reaction I	58.0	72.2	(14.2)	0.76	60.4	(2.4)	0.75	63.0	(5.0)	0.75	54.6	(−3.4)	0.75
d HCOS	stable intermediate	−8.1	−0.8	(7.3)	0.76	−11.7	(−3.6)	0.75	−10.5	(−2.4)	0.75			
e *trans*-HSCO	stable intermediate	−10.0	−3.5	(6.5)	0.77	−14.2	(−4.2)	0.76	−12.8	(−2.8)	0.75	−15.6	(−5.6)	0.76
f *cis*-HSCO	stable intermediate	−7.9	−1.1	(6.8)	0.77	−12.1	(−4.2)	0.75	−10.7	(−2.8)	0.75	−13.5	(−5.6)	0.76
g *trans*-HOCS	stable intermediate	5.2	11.4	(6.2)	0.80	0.9	(−4.3)	0.76	2.7	(−2.5)	0.75	−0.4	(−5.6)	0.76
h *cis*-HOCS	stable intermediate	5.8	12.3	(6.5)	0.80	1.4	(−4.4)	0.76	3.1	(−2.7)	0.75			
i SC···HO	stable intermediate	55.0	68.4	(13.4)	0.76	57.4	(2.4)	0.75	59.9	(4.9)	0.75	51.4	(−3.6)	0.75
j H + OCS → HCOS	H addition/elimination	10.2	12.9	(2.7)	0.82	7.0	(−3.2)	0.76	5.9	(−4.3)	0.76			
l H + OCS → *cis*-HSCO	H-addition/elimination	6.8	9.4	(2.6)	0.85	2.1	(−4.7)	0.76	1.0	(−5.8)	0.76			
n H + OCS → *cis*-HOCS	H addition/elimination	25.1	28.9	(3.8)	0.84	16.5	(−8.6)	0.76	13.6	(−11.5)	0.76			
k *cis*-HSCO → *trans*-HSCO	planar isomerization	10.1	15.9	(5.8)	0.78	2.6	(−7.5)	0.76	2.6	(−7.5)	0.75			
m *cis*-HOCS → *trans*-HOCS	planar isomerization	24.7	30.3	(5.6)	0.79	18.1	(−6.6)	0.76	19.4	(−5.3)	0.75			
q *cis*-HSCO → *trans*-HSCO	nonplanar isomerization	−3.2	3.8	(7.0)	0.79	−6.9	(−3.9)	0.76	−5.7	(−2.5)	0.75			
t *cis*-HOCS → *trans*-HOCS	nonplanar isomerization	15.2	22.6	(7.4)	0.89	10.0	(−5.2)	0.76	11.9	(−3.3)	0.75			
o HCOS → *trans*-HSCO	H-migration	21.5	25.8	(4.3)	0.79	16.8	(−4.7)	0.76	15.5	(−6.0)	0.75			
p HCOS → *trans*-HOCS	H-migration	37.5	43.0	(5.5)	0.80	31.6	(−5.9)	0.76	29.6	(−7.9)	0.75			
v *cis*-HSCO → *cis*-HOCS	H-migration	40.3	45.9	(5.6)	0.76	36.7	(−3.6)	0.75	35.3	(−5.0)	0.75			
r *trans*-HSCO → SH + CO	SH elimination/addition	−7.2	1.3	(8.5)	0.81	−8.6	(−1.4)	0.76				−12.0	(−4.8)	0.77
s *cis*-HSCO → SH + CO	SH elimination/addition	−5.2	3.0	(8.2)	0.81	−7.3	(−2.1)	0.76				−9.7	(−4.5)	0.77
u *trans*-HOCS → SC···HO	OH elimination/addition	55.3	69.6	(14.3)	0.84	58.1	(2.8)	0.75	60.0	(4.7)	0.75	53.3	(−2.0)	0.76

[a] Energy difference from QCISD(T)//UMP26-311+G(2df,2p) value (kcal/mol).

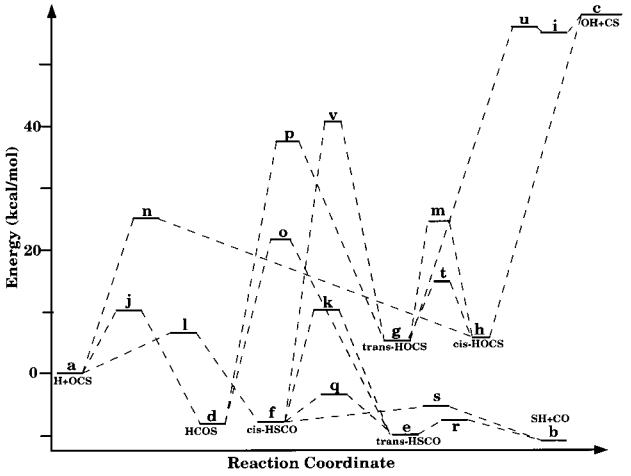

Figure 2. Energy level diagram for the H + OCS potential surface showing the minima and saddle points at the QCISD(T)//UMP2/6-311+G(2df,2p) level. Zero-point energy corrections are included.

estimates the barriers, while MP2 overestimates the barriers. The BLYP predictions were lower than the QCISD(T) values by 4.3 kcal/mol or more. For two of the three hydrogen elimination reactions, both B3LYP and BLYP outperformed UMP2, with B3LYP being within 0.5 kcal/mol of QCISD(T). For the remaining reaction, in which *cis*-HOCS decomposes into H + OCS, UMP2 was in the best agreement with QCISD-(T), followed by B3LYP.

There are two types of isomerization reactions. Transition states **k** and **m** describe the isomerization of the *trans*-HSCO and HOCS species to the cis isomers while keeping the four-body species planar (in-plane isomerization), whereas transition states **q** and **t** describe isomerization to the cis species through an out-of-plane rotation about the X−C (X = S or O) bond (out-of-plane isomerization). For the in-plane isomerizations, UMP2 is in closer agreement with QCISD(T), followed by B3LYP. For the out-of-plane isomerizations, UMP2, B3LYP, and BLYP are all within ∼1.0 kcal/mol of the QCISD(T) barriers. The absolute error of the MP2 predictions for both in-plane (structures **k** and **m**) and out-of-plane isomerization reactions (structures **q** and **t**) is approximately constant and within 1.2 kcal/mol of the QCISD(T) values. The absolute errors of the DFT predictions for the in-plane isomerization reactions are significantly larger than those for the out-of-plane isomerizations and differ from the QCISD(T) results by 2.2−3.3 kcal/mol. Such a distinction suggests that the transition-state structures corresponding to the in-plane isomerizations might have a larger dispersion interaction (which cannot be adequately treated using GGA DFT) than those corresponding to the out-of-plane isomerizations.

For the hydrogen migration reactions, UMP2 and B3LYP are comparable; for some reactions, UMP2 is a slightly better performer, and for others, B3LYP is better. Both levels predict barriers in closer agreement to QCISD(T) than BLYP, which underestimate the barriers by 2.2−5.5 kcal/mol.

Saddle points **r** and **s** corresponding to the SH elimination/addition reactions could not be located at the BLYP level. Also, the prediction of saddle point **r** using the B3LYP functional is questionable. Its energy, without corrections for zero-point energy, is lower than that of the products SH + CO. Also, the magnitude of the imaginary frequency is only 38 cm^{-1}. The distance between the doublet and singlet fragments at the saddle point is 2.8 Å at the B3LYP level, while the UMP2 prediction is 2.3 Å. If corrected for zero-point energy, however, this barrier is 1.6 kcal/mol relative to the products.

For all other barriers associated with diatomic elimination, all three methods give essentially the same results and tend toward overestimating these barrier heights. We have also included the energy differences between the products of reaction I and the OH···CS complex and *cis*-HOCS; these are assumed to proceed without traversing a saddle point. For decomposition of the OH···CS complex, B3LYP is in exact agreement with QCISD(T), followed by BLYP, which is within 0.1 kcal/mol of the QCISD(T). All three levels overestimate the decomposition energy of *cis*-HOCS to form HO + CS by 7−8 kcal/mol, with B3LYP being in closest agreement with QCISD(T).

Finally, for radical SH addition reactions with CO, the UMP2 barrier heights are in closest agreement with QCISD(T), but the DFT predictions of the barrier to formation of *trans*-HOCS from the OH···CS complex are in closer agreement to QCISD-(T) than UMP2 by fractions of a kcal/mol.

TABLE 3: Zero-Point-Corrected Barriers[a] (kcal/mol) for Various Reactions on the H + OCS PES[a]

TS label	description of the reaction	QCISD(T)	MP2	(diff)[b]	B3LYP	(diff)[b]	BLYP	(diff)[b]	BHandHLYP[c]	(diff)[b,c]
				Hydrogen Addition						
j	H + OCS → HCOS	10.2	12.9	(2.7)	7.0	(−3.2)	5.9	(−4.3)		
l	H + OCS → *cis*-HSCO	6.8	9.4	(2.6)	2.1	(−4.7)	1.0	(−5.8)		
n	H + OCS → *cis*-HOCS	25.1	28.9	(3.8)	16.5	(−8.6)	13.6	(−11.5)		
				Hydrogen Elimination						
j	HCOS → H + OCS	18.3	13.7	(−4.6)	18.7	(0.4)	16.4	(−1.9)		
l	*cis*-HSCO → H + OCS	14.7	10.5	(−4.2)	14.2	(−0.5)	11.7	(−3.0)		
n	*cis*-HOCS → H + OCS	19.3	16.6	(−2.7)	15.1	(−4.2)	10.5	(−8.8)		
				Isomerization						
k	*cis*-HSCO → *trans*-HSCO (in-plane)	18.0	17.0	(−1.0)	14.7	(−3.3)	13.3	(−4.7)		
k	*trans*-HSCO → *cis*-HSCO (in-plane)	20.1	19.4	(−0.7)	16.8	(−3.3)	15.4	(−4.7)		
m	*cis*-HOCS → *trans*-HOCS (in-plane)	18.9	18.0	(−0.9)	16.7	(−2.2)	16.3	(−2.6)		
m	*trans*-HOCS → *cis*-HOCS (in-plane)	19.5	18.9	(−0.6)	17.2	(−2.3)	16.7	(−2.8)		
q	*cis*-HSCO → *trans*-HSCO (out-of-plane)	4.7	4.9	(0.2)	5.2	(0.5)	5.0	(0.3)		
q	*trans*-HSCO → *cis*-HSCO (out-of-plane)	6.8	7.3	(0.5)	7.3	(0.5)	7.1	(0.3)		
t	*cis*-HOCS → *trans*-HOCS (out-of-plane)	9.4	10.3	(0.9)	8.6	(−0.8)	8.8	(−0.6)		
t	*trans*-HOCS → *cis*-HOCS (out-of-plane)	10.0	11.2	(1.2)	9.1	(−0.9)	9.2	(−0.8)		
				Hydrogen Migration						
o	HCOS → *trans*-HSCO	29.6	26.6	(−3.0)	28.5	(−1.1)	26.0	(−3.6)		
o	*trans*-HSCO → HCOS	31.5	29.3	(−2.2)	31.0	(−0.5)	28.3	(−3.2)		
p	HCOS → *trans*-HOCS	45.6	43.8	(−1.8)	43.3	(−2.3)	40.1	(−5.5)		
p	*trans*-HOCS → HCOS	32.3	31.6	(−0.7)	30.7	(−1.6)	26.9	(−5.4)		
v	*cis*-HSCO → *cis*-HOCS	48.2	47.0	(0.6)	48.8	(1.8)	46.0	(−2.2)		
v	*cis*-HOCS → *cis*-HSCO	34.5	33.6	(−0.9)	35.3	(0.8)	32.2	(−2.3)		
				Radical Diatomic Elimination						
r	*trans*-HSCO → HS + CO	2.8	4.8	(2.0)	5.6	(2.8)			3.6, 2.6	(0.8, 0.2)
s	*cis*-HSCO → HS + CO	2.7	4.1	(1.4)	3.5	(0.8)			3.8, 3.0	(1.1, 0.3)
u	*trans*-HOCS → OH···CS	50.1	58.2	(8.1)	57.2	(7.1)	57.3	(7.2)	53.7, 55.0	(3.6, 4.9)
no TS	OH···CS → OH + CS	3.0	3.8	(0.8)	3.0	(0.0)	3.1	(0.1)	3.2, 3.9	(0.2, 0.9)
no TS	*cis*-HOCS → OH + CS	52.2	59.9	(7.7)	59.0	(6.8)	59.9	(7.7)		
				Radical Diatomic Addition						
r	SH + CO → *trans*-HSCO	3.4	1.6	(−1.8)	0.4	(−3.0)			3.6, 3.5	(0.2, 0.1)
s	SH + CO → *cis*-HSCO	5.4	3.3	(−2.1)	1.7	(−3.7)			6.2, 6.0	(0.8, 0.6)
u	OH···CS → *trans*-HOCS	0.3	1.2	(0.9)	0.7	(0.4)	0.1	(−0.2)	1.9, 1.5	(1.6, 1.2)

[a] All results calculated using 6-311+G(2df,2p) basis set unless otherwise indicated. [b] Energy difference from QCISD(T) value (kcal/mol). [c] First value corresponds to 6-311+G(2df,2p) result; second value corresponds to 6-31G** result.

Since transition states **r** and **s** were poorly described using the popular BLYP and B3LYP functionals, we investigated whether these points could be better described with a hybrid exchange functional that had a larger contribution from the exact Hartree−Fock than from the B3 functional. This was accomplished using the BHandHLYP density functional given in in the G94 suite of programs. The BHandHLYP/6-311+G(2df,2p) geometric parameters for transition-state structures **r**, **s**, and **u** are given in parentheses in Figure 1, and the relative energies are given in Tables 2 and 3. The BHandHLYP geometries are in closer agreement with the MP2 values, with the largest disagreement being the CO bond in saddle-point structure **u**. The BHandHLYP value is 0.3 Å larger than that from MP2, while the BLYP and B3LYP values are 0.74 and 0.64 Å larger, respectively. Additionally, the COH angle predicted by BHandHLYP is 7° smaller than MP2, while BLYP and B3LYP predictions are 51° and 37° smaller, respectively. We have included the zero-point-corrected BHandHLYP/6-31G** barriers in Table 3. These barriers are within 1.3 kcal/mol of the BHandHLYP/6-311+G(2df,2p) predictions and, with one exception, are closer to the QCISD(T) value than the results found using the larger basis set. This seems contrary to the usual basis set dependence one would expect for a true first-principles calculation.

Conclusions

The work presented here details an investigation into the performance of GGA density functional theory on systems involving radical addition, elimination, and migration reactions. The H + OCS system was chosen for several reasons. First, the PES describes a variety of bonds being made and broken. Second, benchmark data exists in the form of experimental results for several points on the PES and high-level ab initio data[31,32] for these same critical points and the remaining features along the PES. Finally, this is a radical-to-radical reaction, which can pose special problems when treated with the very popular MP2 method due to spin contamination.[50]

This study has two parts. The first compares six DFT functionals using the large aug-cc-pVTZ basis with the experimental values for the heats of reaction for (I) and (II) and the barrier height for the rate-limiting step in (II). The six functionals are BLYP, BP86, B3P86, BPW91, B3PW91, and B3LYP. With the exception of the B3LYP predictions for reaction I, all DFT calculations predict reaction enthalpies that are outside the ranges of experimental measurements. For both reactions, B3LYP/aug-cc-pVTZ is in closest agreement with the measurements and the QCISD(T) predictions. All DFT/aug-cc-pVTZ predictions underestimate both the QCISD(T) formation barrier and the measured activation energy for reaction II. However, three of the DFT predictions (B3LYP, BPW91, and B3PW91) are within 1.7 kcal/mol of the experimental activation energy and 3.5 kcal/mol of the QCISD(T) prediction. BHandHLYP/6-311+G(2df,2p) predictions of the reaction enthalpies for both reactions are closer to experiment and QCISD(T) values than all other DFT predictions.

The second part of the study compared B3LYP and BLYP predictions of properties for all of the critical points located on the PES with the QCISD(T)//UMP2/6-311+G(2df,2p) and UMP2/6-311+G(2df,2p) results. Additionally, a few critical points on the PES were characterized using the BHandHLYP density functional and 6-31G** and 6-311+G(2df,2p) basis sets. The relative energies of the diatomic products are better described by B3LYP than BLYP, BHandHLYP, and UMP2, with BLYP and BHandHLYP outperforming UMP2. With the exception of the weakly bound SC···HO complex, relative energies of the four-body intermediates predicted by BLYP were in closest agreement with QCISD(T), followed by B3LYP, BHandHLYP, and then UMP2. The B3LYP prediction of the energy of the weakly bound SC···HO complex was in the closest agreement to the QCISD(T) predictions.

For 23 out of the 28 barrier heights that were calculated, B3LYP is within 3.7 kcal/mol of the QCISD(T) predictions. Two of the barriers that deviated from QCISD(T) by more than 3.7 kcal/mol were also poorly described by UMP2, and in those cases, B3LYP outperformed UMP2. BLYP barrier height predictions had an overall higher deviation from the QCISD-(T) values than B3LYP or UMP2 but, in some cases, were in very good agreement with the QCISD(T) values. There were two saddle points that could not be located at the BLYP level, one of which was not adequately described by the B3LYP functional. These correspond to elimination or addition of the SH radical from/to the HSCO complex. The same saddle points were optimized using the BHandHLYP density functional and the 6-31G** and 6-311+G(2df,2p) basis sets. Geometric parameters were in better agreement with UMP2 predictions than the B3LYP values. Also, BHandHLYP barrier heights were in closer agreement with QCISD(T) predictions than B3LYP values.

This study shows that DFT outperforms MP2 in predictions of some critical points and that B3LYP is in reasonable agreement with all but one of the ab initio predictions. The erratic behavior of DFT in describing saddle points, including the BHandHLYP density functional, corresponding to radical elimination/addition reactions renders this theoretical method somewhat unreliable for systems such as these. The results of this study suggest that the treatment of transition-state energies with DFT should be approached cautiously, since the results can vary widely with choice of functionals. There appears to be a need for further benchmarking of the existing functionals on the prediction of transition-state energies with ensuing refinements before any can be used with confidence.

Supporting Information Available: Tables giving the geometric parameters and harmonic vibrational frequencies of critical points on the H + OCS PES (7 pages). Ordering information is given on any current masthead page.

References and Notes

(1) Labanowski, J. K.; Andzelm, J. A. *Density Functional Methods in Chemistry*; Springer: Berlin, 1991.

(2) Ziegler, T. *Chem. Rev.* 1991, *91*, 651.

(3) Wang, J.; Johnson, B. G.; Boyd, R. J.; Eriksson, L. A. *J. Phys. Chem.* **1996**, *100*, 6317.

(4) Merrill, G. N.; Kass, S. R. *J. Phys. Chem.* **1996**, *100*, 17465.

(5) Curtiss, L. A.; Raghavachari, K.; Redfern, P. C.; Pople, J. A. *J. Chem. Phys.* **1997**, *106*, 1063.

(6) Rice, B. M.; Chabalowski, C. F. *J. Phys. Chem. A* **1997**, *101*, 8720.

(7) Jursic, B. S. *Chem. Phys. Lett.* **1997**, *264*, 113.

(8) Nguyen, M. T.; Creve, S.; Vanquickenborne, L. G. *J. Phys. Chem.* **1996**, *100*, 18422.

(9) Porezag, D.; Pederson, M. R. *J. Chem. Phys.* **1995**, *102*, 9345.

(10) Baker, J.; Andzelm, J.; Muir, M.; Taylor, P. R. *Chem. Phys Lett.* **1995**, *237*, 53.

(11) Barone, V.; Orlandini, L.; Adamo, C. *Chem. Phys. Lett.* **1994**, *231*, 295.

(12) Johnson, B. G.; Gonzales, C. A.; Gill, P. M. W.; Pople, J. A. *Chem. Phys. Lett.* **1994**, *221*, 100.

(13) Andzelm, J.; Sosa, C.; Eades, R. A. *J. Phys. Chem.* **1993**, *97*, 4664.

(14) Sosa, S.; Lee, C. *J. Chem. Phys.* **1993**, *98*, 8004.

(15) Gronert, S.; Merrill, G. N.; Kass, S. R. *J. Org. Chem.* **1995**, *60*, 488.

(16) Fan, L.; Zeigler, T. *J. Am. Chem. Soc.* **1992**, *114*, 10890.

(17) Basch, H.; Hoz, S. *J. Phys. Chem. A* **1997**, *101*, 4416.

(18) Pai, S. V.; Chabalowski, C. F.; Rice, B. M. *J. Phys. Chem.* **1996**, *100*, 15368.

(19) Mijoule, C.; Latajka, Z.; Borgis, D. *Chem. Phys. Lett.* **1993**, *208*, 364.

(20) Laasonen, K.; Parrinello, M.; Car, R.; Lee, C.; Vanderbilt, D. *Chem. Phys. Lett.* **1993**, *207*, 208.

(21) Kim, K.; Jordan, K. D. *J. Phys. Chem.* **1994**, *98*, 10089.

(22) Hobza, P.; Sponer, J.; Reschel, T. *J. Comput. Chem.* **1995**, *16*, 1315.

(23) Mele, F.; Mineva, T.; Russo, N.; Toscano, M. *Theor. Chim. Acta* **1995**, *91*, 169.

(24) Bytheway, I.; Bacskay, G. B.; Hush, N. S. *J. Phys. Chem.* **1996**, *100*, 6023.

(25) Pudzianowski, A. T. *J. Phys. Chem.* **1996**, *100*, 4781.

(26) Topol, I. A.; Burt, S. K.; Rashin, A. A. *Chem. Phys. Lett.* **1995**, *247*, 112.

(27) Kohn, W.; Meir, Y.; Makarov, D. E. *Phys. Rev. Lett.* **1998**, *80*, 4153.

(28) Pérez-Jordá, J. M.; Becke, A. D. *Chem. Phys. Lett.* **1995**, *233*, 134.

(29) Andersson, Y.; Langreth, D. C.; Lundqvist, B. I. *Phys. Rev. Lett.* **1996**, *76*, 102.

(30) Kristyán, S.; Pulay, P. *Chem. Phys. Lett.* **1994**, *229*, 175.

(31) Rice, B. M.; Chabalowski, C. F. *J. Phys. Chem.* **1994**, *98*, 9488; *J. Phys. Chem.* **1998**, *102*, 3847 (erratum).

(32) Rice, B. M.; Cartland, H. E.; Chabalowski, C. F. *Chem. Phys Lett.* **1993**, *211*, 283.

(33) Frisch, M. J.; Trucks, G. W.; Schlegel, H. B.; Gill, P. M. W.; Johnson, B. G.; Robb, M. A.; Cheeseman, J. R.; Keith, T.; Petersson, G. A.; Montgomery, J. A.; Raghavachari, K.; Al-Laham, M. A.; Zakrzewski, V. G.; Ortiz, J. V.; Foresman, J. B.; Cioslowski, J.; Stefanov, B. B.; Nanayakkara, A.; Challacombe, M.; Peng, C. Y.; Ayala, P. Y.; Chen, W.; Wong, M. W.; Andres, J. L.; Replogle, E. S.; Gomperts, R.; Martin, R. L.; Fox, D. J.; Binkley, J. S.; Defrees, D. J.; Baker, J.; Stewart, J. P.; Head-Gordon, M.; Gonzalez, C.; Pople, J. A. *Gaussian 94*, revision B.1; Gaussian, Inc.: Pittsburgh, PA, 1995.

(34) McLean, A. D.; Chandler, G. S. *J. Chem. Phys.* **1980**, *72*, 5639. Krishnan, R.; Binkley, J. S.; Seeger, R.; Pople, J. A. *J. Chem. Phys.* **1980**, *72*, 650.

(35) Vosko, S. H.; Wilk, L.; Nusair, M. *Can. J. Phys.* **1980**, *58*, 1200.

(36) Becke, A. D. *Phys. Rev. A* **1988**, *38*, 3098.

(37) Becke, A. D. *J. Chem. Phys.* **1993**, *98*, 5648.

(38) Lee, C.; Yang, W.; Parr, R. G. *Phys. Rev. B* **1988**, *37*, 785. Miehlich, B.; Savin, A.; Stoll, H.; Preuss, H. *Chem. Phys. Lett.* **1989**, *157*, 200.

(39) Perdew, J. P. *Phys. Rev. B* **1986**, *33*, 8822.

(40) Perdew, J. P.; Wang, Y. *Phys. Rev. B* **1992**, *45*, 13244.

(41) Dunning, T. H., Jr. *J. Chem. Phys.* **1989**, *90*, 1007. Kendall, R. A.; Dunning, T. H., Jr.; Harrison, R. J. *J. Chem. Phys.* **1992**, *96*, 6796. Woon, D. E.; Dunning, T. H., Jr. *J. Chem. Phys.* **1993**, *98*, 1358.

(42) Tsunashima, S.; Yokota, T.; Safarik, I.; Gunning, H. E.; Strausz, O. P. *J. Phys. Chem.* **1975**, *79*, 775.

(43) Lee, J. H.; Steif, L. J.; Timmons, R. B. *J. Chem. Phys.* **1977**, *67*, 1705.

(44) Nickolaisen, S. L. Ph.D. Dissertation, University of Southern California, 1991.

(45) Wagman, D. D.; Evans, W. H.; Parker, V. B.; Schumm, R. H.; Halow, I.; Bailey, S. M.; Churney, K. L.; Nuttall, R. L. The NBS Tables of Chemical and Thermodynamic Properties. *J. Phys. Chem. Ref. Data, Suppl. 2* **1982**, 11.

(46) Herzberg, G. *Infrared and Raman Spectra of Polyatomic Molecules*; Van Nostrand: Princeton, NJ, 1945. Huber, K. P.; Herzberg, G. *Molecular Spectra and Molecular Structure. IV. Constants of Diatomic Molecules*; Van Nostrand Reinhold: New York, 1979.

(47) Hausler, D.; Rice, J.; Wittig, C. *J. Phys. Chem.* **1987**, *91*, 5413.

(48) Chase, M. W.; Davies, C. A.; Downey, J. R.; Frurip, D. J.; McDonald, R. A.; Syverud, A. N. JANAF Thermochemical Tables 3rd ed. *J. Phys. Chem. Ref. Data, Suppl. 1* **1985**, 14.

(49) Oldershaw, G. A.; Porter, D. A. *J. Chem. Soc., Faraday Trans. 1* **1972**, 68, 709. Oldershaw, G. A.; Smith, A. *J. Chem. Soc., Faraday Trans. 1* **1978**, *74*, 1687.

(50) Bunte, S. W.; Rice, B. M.; Chabalowski, C. F. *J. Phys. Chem. A* **1997**, *101*, 9430.